Int. J. Environ. Sci. Technol. (2015) 12:2649–2664
DOI 10.1007/s13762-015-0776-3

ORIGINAL PAPER

# Adsorption studies of Pb(II) and Cu(II) ions on mesoporous carbon nitride functionalized with melamine-based dendrimer amine

**M. Anbia · M. Haqshenas**

Received: 30 May 2014 / Revised: 30 January 2015 / Accepted: 14 February 2015 / Published online: 10 March 2015

**Abstract** Mesoporous carbon nitride functionalized with melamine-based dendrimer amine has been developed. It has been characterized using $N_2$ adsorption–desorption isotherm, thermogravimetric analysis, Fourier transform spectroscopy and small-angle X-ray scattering techniques. The pore diameter is centered at 4.74 nm with a relatively high BET surface area of 102.2 $m^2/g$ with a pore volume of 0.12 $cm^3/g$. Thermogravimetric analysis curves show that the samples (mesoporous carbon nitride and mesoporous carbon nitride functionalized with melamine-based dendrimer amine) have high thermal stability compared to the earlier species. Batch adsorption experiments were conducted to study the effect of adsorbent dose, temperature, contact time and solution pH for the removal of Pb(II) from aqueous systems. The Pb(II) and Cu(II) removal by mesoporous carbon nitride functionalized with melamine-based dendrimer amine was found to be 196.34 and 199.75 mg/g, respectively. The sorption data are correlated better with the Langmuir adsorption isotherm than Freundlich isotherm. The kinetic analysis has revealed that the overall adsorption process is successfully fitted in the pseudo-second-order kinetic model.

**Keywords** Adsorption · Isotherms · Mesoporous carbon nitride · Pb(II) and Cu(II) · Dendrimer amines

---

M. Anbia (✉) · M. Haqshenas
Research Laboratory of Nanoporous Materials, Faculty of Chemistry, Iran University of Science and Technology, Farjam Street, Narmak, P.O. Box 16846-13114, Tehran, Iran
e-mail: anbia@iust.ac.ir

## Introduction

Many heavy metals enter the environment due to release of industrial effluents. Even at low concentrations, they cause serious pollution problems, threatening people's health. At the same time, some of them such as silver, copper and lead are precious and can be recycled and reused in varied applications (Anbia and Ghassemian 2011). Toxic heavy metals such as Pb(II) and Cu(II) in liquid effluents are considered as persistent, non-biodegradable, bioaccumulative and therefore seriously threaten natural ecosystems and the human health (Amini et al. 2009; Gercel and Gerc 2007; Júnior et al. 2009; Mureseanu et al. 2008). Industries, such as mining and electroplating, discharge aqueous effluents containing high levels of heavy metals like uranium, mercury, cadmium, lead and copper (Reddad et al. 2002; Gavrilescu 2004). Some common techniques for heavy metals removal are chemical precipitation, ion exchange, reverse osmosis, nanofiltration and adsorption (Shahbazi et al. 2011). Most of these methods due to high capital cost are not suitable for small-scale industries. The most effective technique for the removal of environmentally hazardous material is adsorption process. As it is easy to remove the adsorbent from aqueous media after treatment, adsorption technique is generally considered to be an easy method (Yazdankhah et al. 2010). Adsorbents with high surface area are undoubtedly more efficient and have been the topic of the review in this area (Selvam et al. 2011). The common adsorbent material is activated carbon-based adsorbent, which has a large specific surface area, more macro- and micropores, and high adsorption capacity. These adsorbents can be prepared using various low-cost materials that have high carbonaceous content including wood, sawdust, petroleum coke, coal and coconut shell; therefore, they are economically favorable (Bodek et al.

1998). However, the use of activated carbon-based adsorbents, with large fraction of micropores (<2 nm), is limited due to slow diffusion kinetics (Rangel-Mendez and Streat 2002; Wang et al. 2008). Since 1991, synthesis and characterization of nanostructured, mesoporous carbon nitride materials (MCN) have attracted much attention, and significant progress has been made in this area of nanomaterials (Iijima 1991; Lu and Schuth 2005).

In recent years, the incorporation of nitrogen into carbon nanostructures to obtain nitride carbons due to their unique optical, electronic, mechanical and energy storage properties has aroused much attention (Thomas et al. 2008; Kawaguchi et al. 2004; Kroke and Schwarz 2004).Their ability as conductors, precursors of superhard materials, ceramics and their potential applications as catalysts for the selective adsorption of small organic molecules in fuel cells and in dyes have been reported (Jin et al. 2009; Datta et al. 2011; Ansari et al. 2012; Song et al. 2012). They are also used in adsorption and chromatographic separation systems, battery electrodes, nanoreactors, capacitors and biomedical device. Besides the versatility of nanoporous carbon incorporated with nitrogen, they also offer large surface area, high basicity and specific pore volume, in comparison with non-porous nitrogen-doped carbon materials (Vinu et al. 2007a, b; Yang and et al. 2005; Groenewolt and Antonetti 2005).

MCN with two-dimensional pore systems provide access to even wider range of applications because of their unique properties, such as ability to intercalate, semiconductivity, hardness (Qiu and Gao 2003). They have a great potential for application in gas storage, catalysis, lubrication, drug delivery, biomolecule adsorption and fabrication of low dielectric devices. Generally, porous materials have found wide applications (Anbia and Hoseini 2012; Anbia et al. 2010; Anbia and Moradi 2009). There are many reports on the synthesis of non-porous carbon nitride materials (Zimmerman et al. 2001; Gillan 2000; Khabashesku et al. 2000; Kouvetakis et al. 1994). These materials can be synthesized from either chemical or molecular precursors at high temperature. Qiu and Gao (Vinu et al. 2005) have reported the chemical synthesis of non-porous turbostratic carbon nitride materials from polymerized ethylenediamine and carbon tetrachloride. Vinu et al. have reported the synthesis of MCN-1 using SBA-15 as a template (Vinu et al. 2007a, b). However, the surface of the MCN-1 can be improved by functionalization to make it an ideal organic/inorganic hybrid adsorbent. Due to their coordination chemistry and also the binding preferences for metal cations, constrained diffusion of the solution into the pores and also chemical interaction between the MCN-1 surface and the metal cations take place. It is known in the literature that metal cations seek out S–, O– or N– containing organic ligands (Antochshuk and Jaroniec 2002; Olkhovyk and Jaroniec 2005; Jiang et al. 2007). Cu(II) and Pb(II) are the borderline metals with ambivalent properties that show good affinity with aminopropyl-containing ligands. Some workers have used ligands containing multi-amine groups in a chain or ligands involving dendrimer amines to increase removal efficiency of these cations into the NPS pores (Shahbazi et al. 2011).

In 1979, Dendrimers (hyperbranched polymers) were first synthesized by Tomalia and other researchers at the Dow Chemical Corporation (Tomalia et al. 1990). The number of peripheral groups on the chosen branching group allows us to have many functional groups for one covalent bond with MCN surface. Once a proper functional group is attached to the surface of an MCN, one can simply grow the dendrimers off the surface without the necessity of using protecting groups which are usually required in solution dendrimer preparation. An interesting group of dendrimers are those based on 1,3,5-triazine-2,4,6-triamine or melamine. These materials were first synthesized by Eric Simanek's group at Texas A&M in 2000 (Acosta et al. 2004; Zhang and Simanek 2000; Acosta et al. 2005; Zhang and Simanek 2001). The differential reactivity and chemoselective nature of the three reactive sites of 2,4,6-trichloro-1,3,5-triazine (cyanuric chloride) make these dendrimers fairly easy to prepare using diamine linkers and various peripheral groups. Preparation schemes are simplified by manipulating both temperature and sequence of reactions in order to take advantage of the above properties. This approach dramatically reduces the amount of protecting groups required and, in cases where linkers have two dissimilar amine groups, can eliminate the need completely (Zhang and Simanek 2001). This dendritic compound contains a mixture of various amines groups (primary, secondary and tertiary amine groups). These materials are interesting from the perspective that they provide a range of active sites with varied basic strength, rather than a single fixed value. Also, it provides a method for direct adjustment of the surface bound amine concentration per constant unit of pore volume of the substrate (Colilla et al. 2008). Acosta et al. 2004 have synthesized the melamine-based dendrimers using cyanuric chloride as a branching agent and 4-aminomethylpiperidine as the linker. The dendrimer ligands, such as melamine-based dendrimer amines, due to intensively binding amine sites and also to their enhanced hydrophilic MCN surface compared to analogous adsorbents are promising (Shahbazi et al. 2011).

The mesoporous carbon nitride functionalized with melamine-based dendrimer amine (MDA-MCN-1) material, due to the grafted dendrimer amine groups on the surface of MCN-1 and its more active adsorption sites, has good capture selectivity in comparison with MCN species. MDA-MCN-1 with high nitrogen content and due to increase in active adsorption sites has high adsorption capacity for heavy metals (such as Pb, Cu, Cd, Hg) much more than MDA-SBA-15 (Shahbazi et al. 2011).

In this study, MDA-MCN-1 has been synthesized and used to remove Cu(II) and Pb(II) metal ions from aqueous media using batch systems. The effects on the adsorption behavior of the removal process and parameters, such as adsorbent dose, solution pH and temperature, have been studied. Furthermore, Freundlich and Langmuir adsorption isotherms have been studied to explain the sorption mechanism. The kinetics of adsorption of metal ions has also been investigated using pseudo-first- and pseudo-second-order kinetics models.

## Materials and methods

### Chemicals and reagents

All the chemicals used were of analytical grade from E. Merck (Germany), except poly(ethylene oxide)–poly(propylene oxide)–poly(ethylene oxide) block copolymer nonionic surfactant EO20PO70EO20 (Pluronic P123) which was supplied by Aldrich (UK).

### Synthesis of mesoporous silica SBA-15

Mesoporous silica SBA-15 was prepared by the hydrothermal method using tetraethyl orthosilicate (TEOS) as silica precursor, Pluronic P123 as template and $H_3PO_4$ to make the media acidic. Briefly, P123 block copolymer (4 g) was dissolved in $H_3PO_4$ (9 g) inside beaker by stirring with magnet for 5 h at room temperature. Then, TEOS (9.6 mL) was slowly (drop by drop) added to that solution and stirred for 24 h at 40 °C. The mixture was then aged in a sealed glass bottle at 100 °C for 24 h under static conditions. The mixture was then allowed to cool at room temperature, and the white solid product was filtered by Büchner funnel, washed with distilled water for removing extra surfactant and then dried in air. The solid was calcined in a two-step procedure based on heating first at 25 °C for 3 h and then at 550 °C for 4 h (Anbia and Parvin 2011). White precipitate was obtained. Complete surfactant removal was confirmed in all cases using thermogravimetric analysis, and a white powder (SBA-15) was obtained (Chew et al. 2010).

### Synthesis of MCN-1

In a typical synthesis, 0.5 g of calcined SBA-15 was added to the mixture of ethylenediamine (2.2 g) and carbon tetrachloride (5.4 g). The resultant mixture was refluxed and stirred at 90 °C for 6 h (Vinu et al. 2007a, b). Then, the dark-brown solid mixture obtained was moved to watch glass and then was placed in a drying oven for 12 h and after that was grounded into a fine powder. The template carbon nitride polymer composites (dark-brown precipitate) were then heat-treated in a nitrogen flow at 600 °C with a heating rate of 3.0 °C/min and was kept under these conditions for 5 h to carbonize the polymer inside nitrogen furnace (Zheng et al. 2010). The mesoporous carbon nitride was recovered after dissolution of the silica framework in 5 wt% hydrofluoric acid, followed by filtration by Büchner funnel and washing several times with ethanol and then drying at 100 °C (Kouvetakis et al. 1994). Black precipitate was obtained.

### Synthesis of MDA-MCN-1

The MDA-MCN-1 was synthesized from cyanuric chloride and ethylenediamine (EDA) according to a procedure similar to that described previously in the literature. Cyanuric chloride (5.5 g) and diisopropylethylamine (DIPEA) (7.1 mL) were dissolved in dried tetrahydrofuran (300 mL) and stirred at 0 °C for 3 h under argon atmosphere. MCN was added to the mixture and stirred for 24 h at 0 °C. The chlorine atom in cyanuric chloride was easily replaced by the amine group of the EDA molecule, and the DIPEA trap that HCl formed during the substitution reaction. Then, the mixture was filtered by Büchner funnel, and the solid was rinsed sequentially by dried methanol, dichloromethane and tetrahydrofuran (Liang et al. 2008). The solid was transferred back into a clean flask containing a mixture of EDA (4 mL), dissolved in dried tetrahydrofuran (300 mL) and refluxed for 24 h at 0 °C. The material was filtered by Büchner funnel and rinsed by dried methanol, dichloromethane and tetrahydrofuran, in sequence. This black precipitate obtained is referred as MDA-MCN-1 (Shahbazi et al. 2011). Figure 1 shows schematic illustration of synthesis of MCN-1 functionalized by melamine-based dendrimers amine (MDA-MCN-1).

### Characterization of adsorbents

Nitrogen sorption isotherms were measured with a Micromeritics 2020 analyzer at 77 K. Before measurements, the samples were degassed at 90 °C in a vacuum for 3 h. The Brunauer–Emmett–Teller (BET) method was utilized to calculate the specific surface areas (SBET). The pore size distributions were calculated from the adsorption branches of isotherms using the Barrett–Joyner–Halenda (BJH) model. The total pore volumes (Vt) were estimated from the adsorbed amount at a relative pressure P/P0 of 0.99. A thermogravimetric analyzer (NETZSCH TG 209 F1, Iris) was used to determine the thermal stability of materials in nitrogen atmosphere with a heating rate of

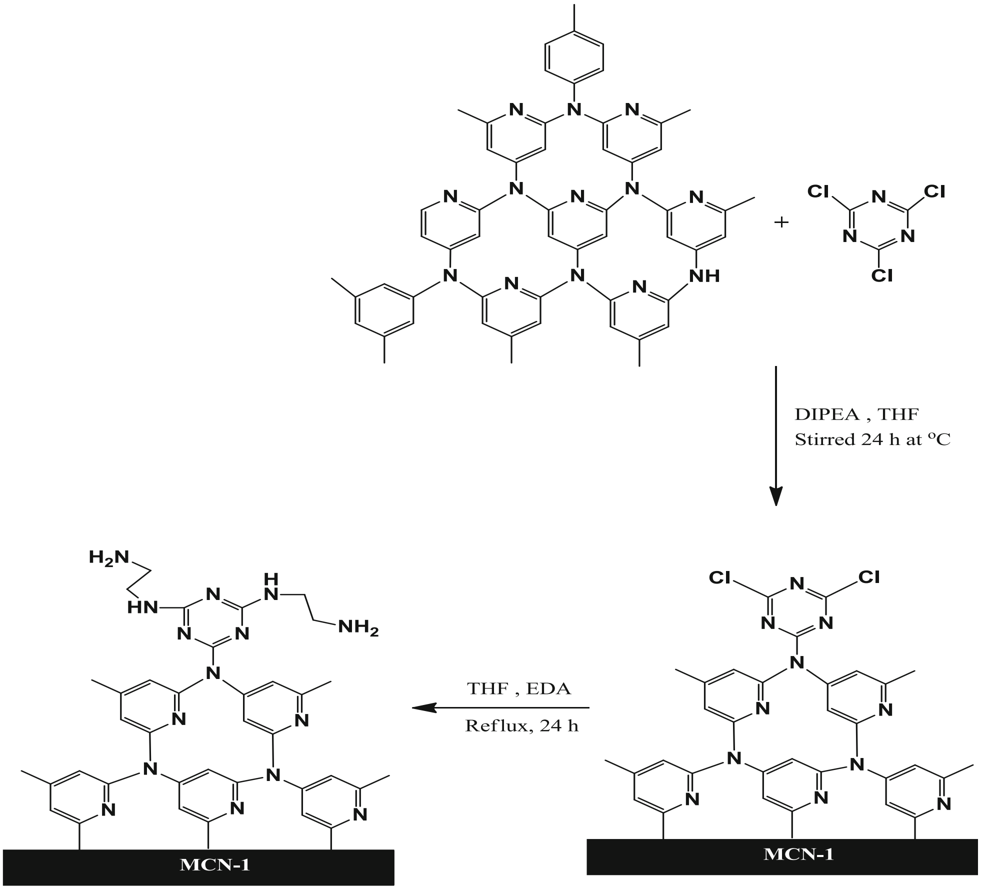

**Fig. 1** Schematic illustration of synthesis of MCN-1 functionalized by melamine-based dendrimers amine (MDA-MCN-1)

10.0 K/min. X-ray scattering (SAXS) measurements were carried out on a Hecus SAXS system (model S3-MICRO-pix) using Cu-K$_\alpha$ radiation (50 kV, 1 mA). Fourier transform (FTIR) spectra of the samples were measured on a Shimadzu IR solution 8400 spectrometer using the usual KBr pellet technique.

## Adsorption studies

Adsorption experiments were performed in 100-mL conical flasks containing 25 mL of single metal nitrate solution, stirring at 25 °C with 150 rpm. The equilibrium study was carried out by sampling at regular intervals of 0.5 min. In the present study, a contact time of 5 and 7 min for Cu(II) and Pb(II), respectively, was required to reach equilibrium. Therefore, we used 20-min contact time for all further experiments. In each sample, the adsorbent was separated with Whatman No. 50 filter papers to collect the final solutions (Anbia and Ghassemian 2011). Stock solutions of each Pb(II) and Cu(II) ions were prepared by dissolving exact amounts of $Pb(NO_3)_2$ and $Cu(NO_3)_2$ in de-ionized water. The concentration of the metal ions in the solution was measured using atomic absorption spectrophotometer (Shimadzu, AA-6300, Japan). The removal efficiency of the metal ions was calculated by the following equation:

$$R = \frac{C_0 - C_t}{C_0} \tag{1}$$

where $R$ is the removal efficiency of the metal ion, $C_0$ the initial concentration, and $C_t$ the concentration of the metal ion in mg/L at $t$ in time. The adsorption capacity of the adsorbent (metal uptake) at equilibrium was also calculated by the following equation (Yuan et al. 2007):

$$q_e = \frac{(C_0 - C_e)}{W} \tag{2}$$

where $q_e$ is the equilibrium adsorption capacity of the adsorbent in mg/g, $C_0$ is the initial concentration in mg/L, $C_e$ are the concentration at equilibrium of metal ions in mg/L, $V$ is the volume in L of metal ions solution, and $W$ is the weight in g of the adsorbent. The experiments were done in duplicate, and the average values were reported.

## Effect of the adsorbent dose

In the adsorption studies, the effects of the dose of MDA-MCN-1 (0.5, 1, 1.5, 2, 2.5, 3.5 g/L) adsorbents on adsorption of Pb(II) and Cu(II) metal ions with 100 mg/L at room temperature for 20 min contact time were studied. The pH of the working solution was adjusted to 5 by adding 0.1 M NaOH. The conical flasks were agitated at 150 rpm using a mechanical shaker to reach equilibrium (Abdel-Ghani and Elchaghaby 2007). After filtration, the concentration of the remaining metal ions in aqueous phase was measured.

### Effect of the solution pH

The effects of the different initial solution pH on adsorption were studied by mixing 2 and 4.5 g/L of MDA-MCN-1 for Cu(II) and Pb(II) in 25 mL of a single solution containing 100 mg/L of Pb(II) and Cu(II) metal ions. The pH was adjusted to values ranging from 1 to 13 using 1 M HCl and 0.1 M NaOH solution. The conical flasks were agitated at 150 rpm using a mechanical shaker to reach equilibrium (Anbia and Ghaffari 2009). After filtration, the concentration of the remaining metal ions in aqueous phase was measured.

### Effect of temperature

The effects of temperature (20, 30, 40 °C) on metal ions adsorption were conducted with 2 and 4.5 g/L of MDA-MCN-1 as adsorbent dose for Cu(II) and Pb(II) in 25 mL of single metal ion solution at pH 8, each containing 100 mg/L of Pb(II) and Cu(II) (Zvinowanda et al. 2009). The conical flasks were agitated at 150 rpm using a mechanical shaker to reach equilibrium. After filtration, the concentration of the remaining metal ions in aqueous phase was measured.

### Adsorption isotherms

The adsorption isotherm studies were performed at equilibrium conditions, in order to determine the relationship between the amount of metal ions adsorbed on the adsorbent surface and the concentration of remaining metal ions in the aqueous phase. These adsorption data for each Pb(II) and Cu(II) metal ions were fitted into both the Freundlich and Langmuir isotherm equations. The Langmuir isotherm is based on the monolayer sorption of metal ions on the surface of the sorbent and is represented by the following equation (Anbia and Habibi Davijani 2013):

$$\frac{C_e}{q_e} = \frac{1}{q_m b} + \left(\frac{1}{q_m}\right) C_e \qquad (3)$$

where $q_e$ is the equilibrium adsorption capacity of the sorbent in mg/g and $C_e$ is the concentration of metal ions in mg/L at equilibrium. The $q_m$ is the maximum capacity of the metal monolayer to be adsorbed in mg/g, and b is the constant that refers to the bonding energy of adsorption in L/mg.

The Freundlich isotherm model is considered to be appropriate for describing both multilayer sorption and sorption on heterogeneous surfaces. The Freundlich model can be expressed by the following equation (Anbia and Habibi Davijani 2013):

$$\ln q_e = \ln K_f + \left(\frac{1}{n}\right) \ln C_e \qquad (4)$$

where $q_e$ is the equilibrium adsorption capacity of the adsorbent in mg/g, $C_e$ is the concentration of heavy metal ions in mg/L at equilibrium, $K_f$ is the constant related to the adsorption capacity of the adsorbent, and $n$ is the empirical constant related to the intensity of adsorption which varies with the heterogeneity of the adsorbent. The greater the value of $n$, the more favorable it is for adsorption.

Temkin isotherm is represented by the following equation (Anbia and Habibi Davijani 2013):

$$q_e = B \ln k_t + B \ln C_e \qquad (5)$$

where $K_t$ is the equilibrium binding constant (L/mg) corresponding to the maximum binding energy and the $B$ constant is related to the heat of adsorption.

### Adsorption kinetics

For the measurement of the time-resolved uptake of Pb(II) and Cu(II) on the adsorbents, 25 mL of distilled water was mixed with 2 and 4.5 g/L of adsorbent for Cu(II) and Pb(II) in a 100-mL flask. Pb(II) and Cu(II) solutions were quickly introduced into the flask (keeping the initial concentrations of the resulting solutions at 100 mg/L) and stirred continuously at 20 °C. Sampling was done by fast filtration at different time intervals.

The concentration of residual Cu(II) and Pb(II) in the solution was determined, and the adsorption amount $q_f$ was calculated according to Eq. (6):

$$q_t = \frac{(C_0 - C_t)V}{W} \qquad (6)$$

where $q_t$ is the adsorption amount at time $t$, $C_0$ is the initial concentration of Cu(II) and Pb(II) solution, $C_t$ is the concentration of Cu(II) and Pb(II) solution at time $t$, $V$ is the volume of Cu(II) and Pb(II) solution, and $W$ is the mass of mesoporous materials (Anbia and Habibi Davijani 2013).

## Results and discussion

### Structural and textural properties

The FTIR spectrum of the MCN-1 material shows three major bands at 1276, 1606 and 3406 $\text{cm}^{-1}$ (Fig. 2a): The bands at 1276 and 1606 $\text{cm}^{-1}$ are assigned to aromatic C–

N stretching bonds and aromatic ring modes, respectively, while the broad peak at 3406 $cm^{-1}$ is attributed to the stretching mode of N–H groups in the aromatic ring (Acosta et al. 2005). The bands at 2864 and 2902 $cm^{-1}$ correspond to terminal $CH_3$ groups. A shoulder at 1417 $cm^{-1}$ is assigned to a $sp^3$ C–C bond or disordered $sp^2$ graphitic domains, and bonds below 933 $cm^{-1}$ to graphitic $sp^2$ domains (Qiu and Gao 2003). The FTIR spectrum of MDA-MCN-1 is also shown in Fig. 2a. The bands at 1434 and 1546 $cm^{-1}$ (MDA-MCN-1 spectrum) are due to an aromatic triazine ring in the MDA-MCN-1 sample and confirm that the MDA is formed (Shahbazi et al. 2011). The IR bands at 3415 and 3467 $cm^{-1}$ are due to asymmetric and symmetric $NH_2$ stretching. MDA-MCN-1 spectra reveal new bands at ~1649 and ~1544 $cm^{-1}$, which are attributed to the C=N stretching in the triazine ring. N–H stretching bands can be observed at 3124–3500 $cm^{-1}$. The bands at 2813 and 2661 $cm^{-1}$ correspond to $CH_2$ groups (Liang et al. 2008).

The nitrogen adsorption isotherms of MCN-1 and MDA-MCN-1 samples are shown in Fig. 2b and are of type IV according to the International Union of Pure and Applied Chemistry (IUPAC), indicating that the synthesized samples are mesoporous compounds. The samples exhibit a total pore volume of 0.12 and 0.53 $cm^3/g$ and a specific BET surface area of 102.24 and 505.65 $m^2/g$ for MDA-MCN-1 and MCN-1, respectively. The modified BJH adsorption and desorption pore size distribution (4 V/A) of MDA-MCN-1 are compared to MCN-1. The adsorption and desorption pore size distribution of MCN-1 are centered at 4.48 nm, and the adsorption and desorption pore size distribution of MDA-MCN-1 are centered at about 2.4 and 7 nm. Table 1 shows the effective mesopore diameter increase as the dendrimer is formed inside the mesopore. This abnormal increase in the diameter after the functionalization with amine group (from 4.23 to 4.74 nm for functionalization with melamine dendrimer) is due to either the stereo effect or the channel blocking by amino group

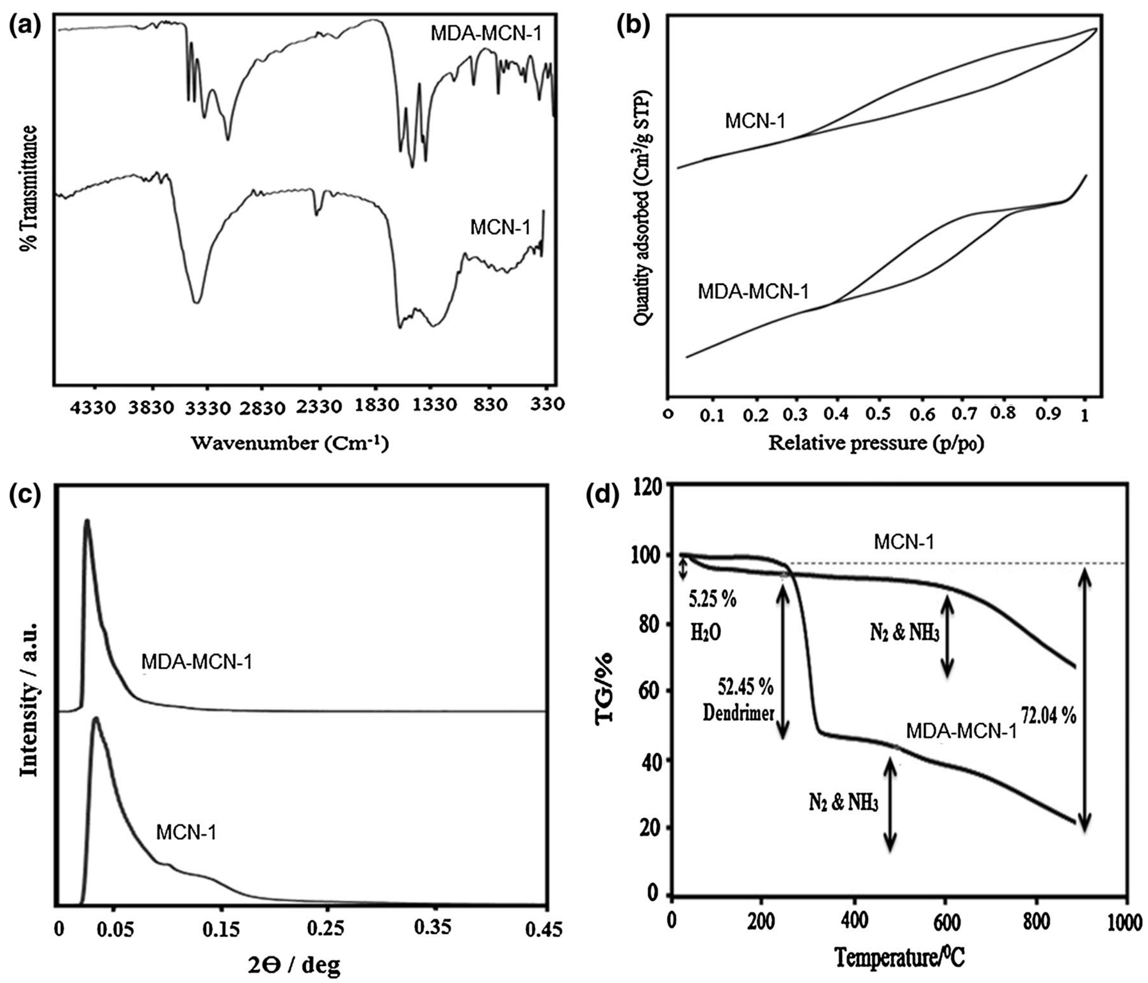

**Fig. 2** Characterization of adsorbents; **a** FTIR spectra, **b** nitrogen adsorption–desorption isotherms, **c** SAXS patterns, and **d** thermogravimetric curves

**Table 1** BET surface area ($S_{BET}$), mean pore diameter and total pore volume from $N_2$ adsorption–desorption isotherms for the synthesized adsorbents (MCN-1 and MDA-MCN-1)

| Molecular sieves | SBET ($m^2/g$) | Mean pore diameter (nm) | Total pore volume ($m^2/g$) |
|---|---|---|---|
| MDA-MCN-1 | 102.2 | 4.74 | 0.12 |
| MCN-1 | 505.6 | 4.2 | 0.53 |

(Chew et al. 2010). It is also interesting that there is a dramatic decrease in the volume adsorbed (0.12 $cm^3/g$) for MDA-MCN-1 as compared to the MCN-1 (about 0.53 $cm^3/g$).

The SAXS spectra for MCN-1 and MDA-SBA-15 are shown in Fig. 2c. Both synthesized adsorbents exhibit a singles strong peak (1 0 0) on its XRD pattern followed by two additional peaks (1 1 0, 2 0 0) which can be indexed on a hexagonal lattice. The pattern is similar to the XRD pattern of the parent mesoporous silica template SBA-15, although some peak broadening was observed as compared to the parent SBA-15 (Colilla et al. 2008). Consequently, the bonding of the MDA complexes inside the mesoporous channels of MCN-1 does not seriously perturb the overall ordered structure of the MCN.

The thermogravimetric analysis (TGA) curves of two samples are recorded in Fig. 2d. Organic loadings in the MCN-1 and MDA-MCN-1 sample were calculated from the weight loss determined by TGA. The negligible mass loss between 25 and 100 °C is about 5.25 % of MCN-1-associated desorption of water. The significant mass loss about 52.45 % of MDA-MCN-1 material occurs at 305 °C, which can be attributed to the decomposition of dendrimer partition of the sample. The main decomposition of MCN-1 starts at around 600 °C, which is related to the release of small molecules including $N_2$ and $NH_3$ of the samples. This step of destruction for MDA-MCN-1 was observed at about 470 °C and shows loss of thermal stability for MDA-MCN-1 compared with MCN-1. As can be observed up to a temperature of about 900 °C, only 72.04 % of the MDA-MCN-1 is lost. This result shows that samples (MCN-1 and MDA-MCN-1) have high thermal stability compared to earlier species.

## Adsorption of Pb(II) and Cu(II) metal ions

### *Effect of contact time*

In order to establish equilibration time for maximum uptake and to know the kinetics of the adsorption process, the adsorption of Pb(II) and Cu(II) on MDA-MCN-1 was studied as a function of contact time, and the results are shown in Fig. 3. This figure indicates that the time required for equilibrium adsorption is around 5 and 7 min for Cu(II) and Pb(II), respectively. Thus, for all equilibrium adsorption studies, the equilibration period was kept 20 min.

### *Effect of temperature*

Effect of temperature on adsorption capacity ($q_e$) of heavy metals onto MDA-MCN-1 at different temperatures is shown in Fig. 4. Temperature is a highly significant parameter in the adsorption process. As it can be seen from the figures, decrease in temperature generally increases the adsorption capacity and maximum adsorption capacity is noticed at 20 °C. Adsorption is nearly always a diffusion process with exothermic nature. High temperature can result in an increase in the mobility of the acidic compounds but can decrease the interaction of heavy metals with active sites of MDA-MCN-1, which causes a decrease in adsorption capacity.

In order to gain an insight into the mechanism involved in the adsorption process, thermodynamic parameters for

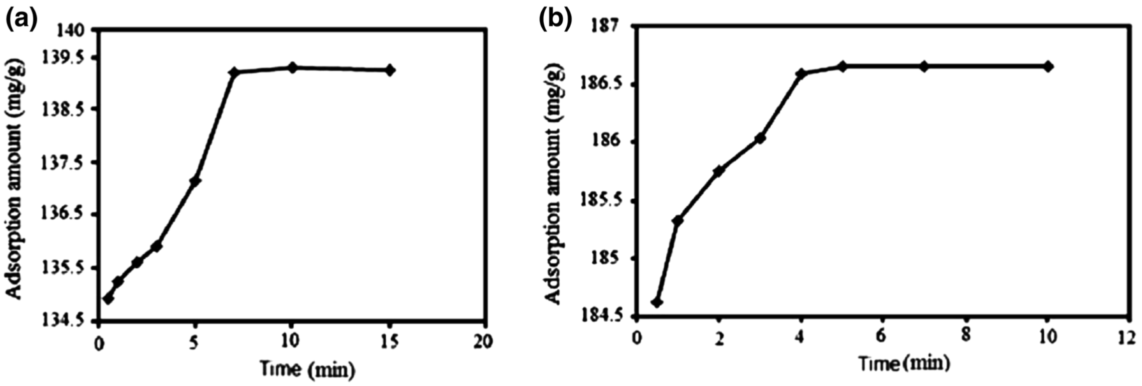

**Fig. 3** Effect of contact time on removal of **a** Pb(II) [pH = 8, [Pb(II)] = 100 mg/L, agitation speed = 150 (rpm), adsorbent dosage = 4.5 g/L, room temperature = 20 °C] and **b** Cu(II) [pH = 8, [Cu(II)] = 100 mg/L, agitation speed = 150 (rpm), adsorbent dosage = 2 g/L, temperature = 20 °C]

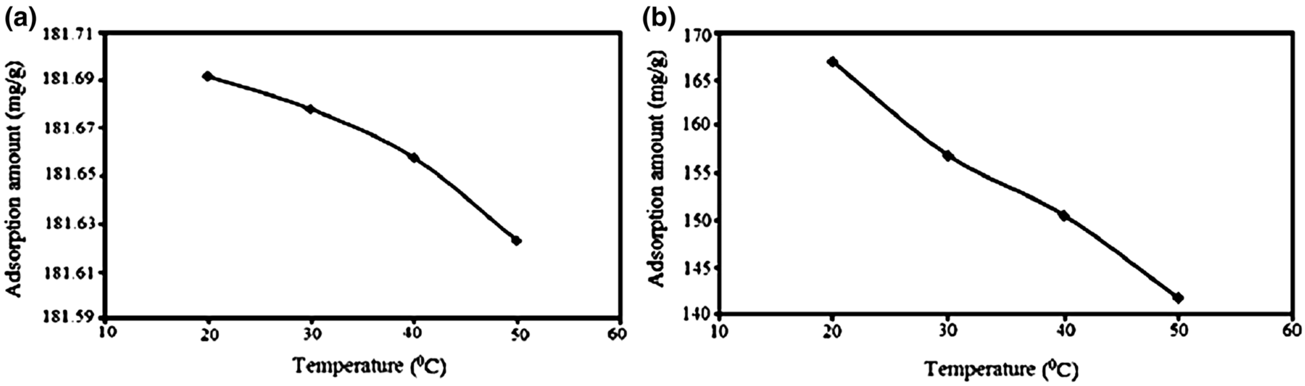

**Fig. 4** Effect of temperature on removal of **a** Cu(II) [pH = 8, [Cu(II)] = 100 mg/L, agitation speed = 150 (rpm), adsorbent dosage = 2 g/L, room temperature = 20 °C] and **b** Pb(II) [pH = 8, [Pb(II)] = 100 mg/L, agitation speed = 150 (rpm), adsorbent dosage = 4.5 g/L, room temperature = 20 °C]

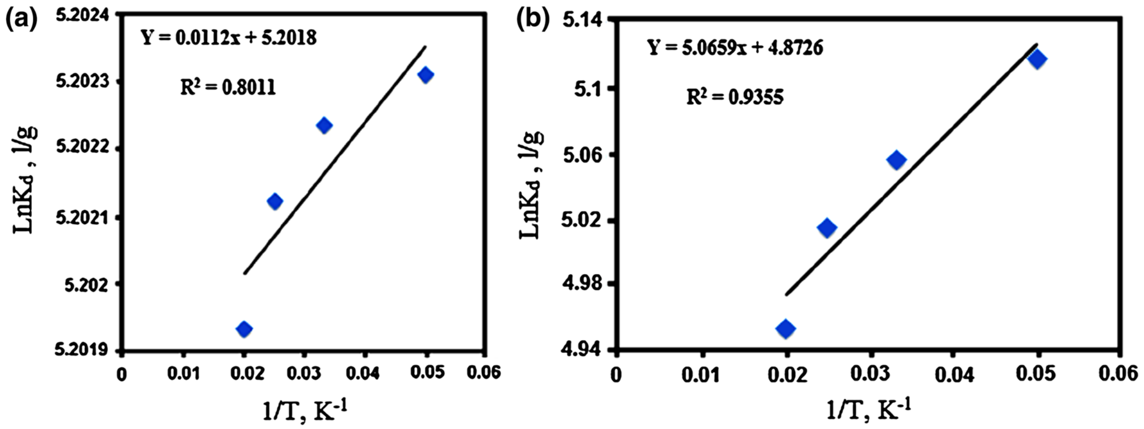

**Fig. 5** Plots of ln $k_d$ versus 1/T for **a** Cu(II) and **b** Pb(II) adsorption on MDA-MCN-1

the present system were calculated. The Gibbs free energy ($\Delta G^0$), adsorption enthalpy ($\Delta H^0$) and adsorption entropy ($\Delta S^0$) at different temperatures were calculated using the following thermodynamic functions (Shahbazi et al. 2011):

$$\ln K_d = \frac{\Delta S^0}{R} - \frac{\Delta H^0}{RT} \tag{7}$$

where the values of $\Delta S^0$(change in entropy in J/mol K) and $\Delta H^0$(change in enthalpy in J/mol) are obtained from the slope and intercept of ln $K_d$ versus $1/T$ plots. $T$ is the temperature in $K$, and $R$ is the universal gas constant (8.314 J/mol K). The distribution coefficient ($k_d$) is calculated from the equilibrium and the initial concentrations ($C_e$ and $C_0$) of the metal ions,

$$K_d = \frac{C_0 - C_e}{C_e} \times \frac{V}{W} \tag{8}$$

where $W$ is the adsorbent mass in $g$ and $V$ is the working volume in mL. $\Delta G^0$ is the change in Gibbs free energy in J/mol, calculated according to the following equation (Shahbazi et al. 2011):

$$\Delta G^0 = \Delta H^0 - T\Delta S^0 \tag{9}$$

The effect of temperature on the adsorption of heavy metal ions onto MDA-MCN-1 is shown by the linear plot of ln $K_d$ versus $1/T$ in Fig. 5, and the relative parameters and correlation coefficients calculated from Eqs. (7–9) are listed in Table 2. The negative values of $\Delta H^0$ and the decreasing value of $k_d$ with increasing temperature indicate that the sorption of Pb(II) and Cu(II) and Cd(II) onto the MDA-MCN-1 is an exothermic process. The exothermic nature of adsorption is probably due to an existence of a high number of adsorption sites on the surface of adsorbent so that they improve metal ions adsorption. The results also show that the Gibbs free energy change is less at a lower temperature, indicating more feasibility of the adsorption process, and it is becoming higher with increasing temperature, indicating that sorption is less positive at high temperatures. Thus, the thermodynamic study reveals that the adsorption process of heavy metal ions has a spontaneous nature and is promoted by decreasing the temperature from 50 to 20 °C.

**Table 2** Thermodynamic parameters of Pb(II), Cu(II) and Cd(II) adsorption on MDA-SBA-15 at different temperatures in Kelvin (initial concentration of metal ion 100 mg/L)

| Heavy metals | Δ*H* (J/mol) | Δ*S* (J/mol K) | Δ*G* | | | |
|---|---|---|---|---|---|---|
| | | | 293 $K^0$ | 303 $K^0$ | 313 $K^0$ | 323 $K^0$ |
| Pb(II) | −42.12 | 40.51 | 11,911.55 | 12,316.65 | 12,721.75 | 13,126.847 |
| Cu(II) | −0.0931 | 43.247 | 12,671.46 | 13,060.69 | 13,536.60 | 13,968.87 |

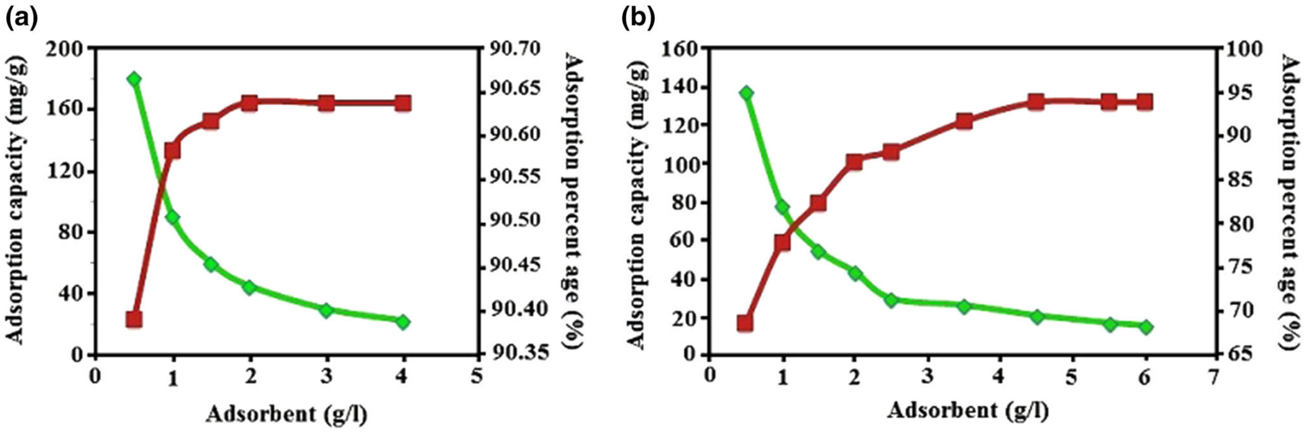

**Fig. 6** Effect of MDA-MCN-1 amount on the adsorption of **a** Cu(II) [pH 8, [Cu(II)] = 100 ppm, agitation speed = 150 (rpm), temperature = 20 °C] and **b** Pb(II) [pH 8, [Pb(II)] = 100 ppm, agitation speed = 150 (rpm), temperature = 20 °C]

### *Effect of adsorbent dose*

Adsorbent dose is also an important parameter in determination of adsorption percentage and adsorption capacity. Figure 6 shows adsorption capacity and adsorption percentage of heavy metals. The results suggest that at constant concentration of heavy metals by increasing the adsorbent contents, the adsorption percent increases, but adsorption capacity decreases. An increase in adsorption percent can be attributed to increased surface area and consequential increase in interference between binding sites at the higher dose or insufficiency of metal ions in solution with respect to available binding sites, whereas the decrease in adsorption capacity is due to the fact that some of the adsorption sites remain unsaturated during the adsorption process. The maximum metal ions removal was attained at about 2 and 4.5 g/L dose of MDA-MCN-1 for Cu(II) and Pb(II), respectively, and was almost the same even at higher doses.

### *Effect of pH*

The effect of the solution pH can be associated with a number of mechanisms such as metal speciation in solution, changes of the ionic forms of the functional groups on the adsorbent surface and the competitive effects of hydrogen ions with metal ions. Therefore, a study was conducted in order to optimize the pH when other parameters such as dose of MDA-MCN-1, concentration of metal ions and temperature were kept constant. Figure 7 shows the effect of the pH on the removal efficiency of Pb(II) and Cu(II) as the function of the solution pH, obtained with the initial metal concentration of 100 mg/L and 4.5 and 2 g/L MDA-MCN-1, respectively. The metal uptake increases while increasing the pH from 1 to 2 for Cu(II) and Pb(II) till it reaches a maximum at 8, and then decreases at the pH value higher than 8. As shown in Fig. 7a, b, the adsorption amount was 82.64 and 181.17 mg/L at pH 2 and 1 for Pb(II) and Cu(II), respectively, and these values increased to 196.34 and 199.75 mg/L for Pb(II) and Cu(II), respectively, with pH increasing to 8. This is because at low pH values, there is an excessive protonation of the lone pair of electrons on nitrogen, resulting in a decrease in the sorption of heavy metal ions (Benhamou et al. 2009; Heidari et al. 2009). Also, at a very low solution pH, the concentration of the hydrogen ions is high, directly competing with the heavy metal ions for active binding sites. Therefore, the increase in metal removal as the pH increases can be explained on the basis of a decrease in competition between proton ions ($H^+$) and positively charged metal ions at the adsorbent surface sites. The maximum adsorption was observed at pH 8 for both of them. However, on increasing the pH further, the metal speciations in solution may become an important

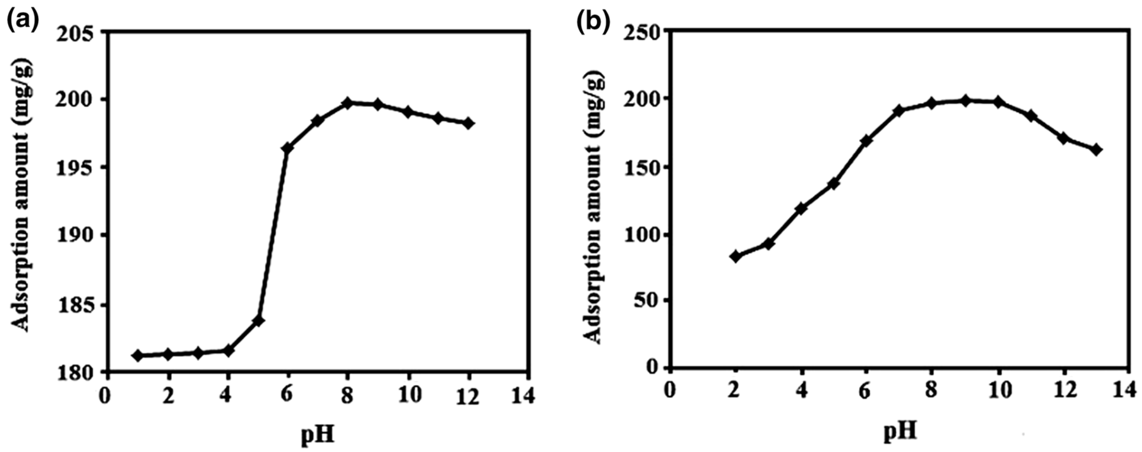

**Fig. 7** Effect of pH on heavy metals removal by MDA-MCN-1 **a** [Cu(II) = 100 mg/L, adsorbent dose = 2 g/L, agitation speed = 150 rpm, temperature = 20 °C] and **b** [Pb(II) = 100 mg/L, adsorbent dose = 4.5 g/L, agitation speed = 150 rpm, temperature = 25 °C]

factor and the increase in heavy metal removal has been attributed to reduced solubility and precipitation of solid metal hydroxide.

When the pH increased from 8 to higher value, the removal efficiency of ions was decreased because of ion precipitation. To explain this observation, the presence of dominant metal ions M(II) species at $\text{pH} > 8$ is $M(OH)_2$ and at $\text{pH} < 8$ is $M^{2+}$ and $M(OH)^+$; therefore, most ions are not accessible to adsorb at higher pH values, and consequently, the removal efficiency decreased.

The mechanism of Pb and Cu retention on MDA-MCN-1 can be described by the adsorption reactions as following expressions:

(a) $\mathrm{C{-}NH + M^{2+} \rightarrow A{-}N{-}M^{+} + H^{+}}$

(b) $\mathrm{C{-}NH + MOH^{+} \rightarrow A{-}N{-}M(OH) + H^{+}}$

The point of zero charge ($\text{pH}_{\text{zpc}}$) plays an important role in the adsorption process. Anionic adsorption is favored at $\text{pH} < \text{pH}_{\text{zpc}}$, and cationic adsorption is favored at $\text{pH} > \text{pHzpc}$. The $\text{pH}_{\text{zpc}}$ of MDA-MCN-1 was found to be about 6.2. At pH above $\text{pH}_{\text{zpc}}$, the surface of mesoporous carbon is negative, and there is a strong electrostatic attraction between surface groups and Pb(II) and Cu(II) species. As a result, above $\text{pH}_{\text{zpc}}$, the adsorption of Pb(II) and Cu(II) was reached maximum at pH. At pH values less than $\text{pH}_{\text{zpc}}$, the carbon surface is positively charged resulting in lower adsorption due to electrostatic repulsion between the positive surface charge of mesoporous carbon and $Pb^{2+}$ and $Cu^{2+}$ (Zolfaghari et al. 2011).

For example, copper ion speciation is affected by solution pH through the following equilibrium:

$$\mathrm{Cu^{2+} + OH^{-} = Cu(OH)^{+}pK_{1} = -6}$$

$$\mathrm{Cu(OH)^{+} + OH^{-} = Cu(OH)_{2}pK_{2} = -12.8}$$

(1) When $\text{pH} > \text{p}K_a$ $[H^+ < K_a]$, the deprotonated hydrolysis product is the dominant species present in the solution. (2)When $\text{pH} < \text{p}K_a$ $[H^+ > K_a]$, the hydrated species is the dominant species present in the solution. (3) When $\text{pH} = \text{p}K_a$, the hydrated species and hydrolysis product have equal activities in solution $[\text{p}K_1 : Cu^{2+} = Cu(OH)^+$ and $\text{p}K_2 : Cu(OH)^+ = Cu(OH)_2]$. The adsorption of copper slightly increased between pH 1 and 4 and more rapidly increased at higher pH especially near of 6 that concentration of $Cu^{2+}$ and $Cu(OH)^+$ are equal, increasing is more and reach a maximum at pH 8. At $\text{pH} > \text{p}K_2$, copper was mainly present as $Cu(OH)_2$ that were precipitated.

### *Adsorption isotherms*

Adsorption isotherms are characterized by certain constant values, which express the surface properties and affinity of the adsorbent and can also be used to compare the adsorption capacities for metal ions. The isotherm data have linearized using the Langmuir and Freundlich equation. The $b$, $q_m$, $n$, $K_f$ values and the linear regression correlation coefficients ($R^2$) for Langmuir and Freundlich isotherms are given in Table 3. The correlation coefficients indicate that adsorption was fitted better by the Langmuir ($R^2 = 0.95$–$0.99$) than the Freundlich model ($R^2 = 0.71$–$0.87$) and Temkin model ($R^2 = 0.79$ and $R^2 = 0.9999$). Langmuir isotherm is shown in Fig. 8. Therefore, the adsorption process can be described due to the formation of a monolayer coverage of the adsorbate on the adsorbent surface. The Freundlich isotherm interprets adsorption on heterogeneous surfaces or to surfaces supporting sites of varied affinities. In this study, at first the amine adsorption sites in melamine groups with strong

**Table 3** Langmuir, Freundlich and Temkin parameters for the adsorption of Pb(II) and Cu(II) in single solutions onto MDA-MCN-1

| Metals | Langmuir | | | Freundlich | | | Temkin | | |
|---|---|---|---|---|---|---|---|---|---|
| | $q_m$ (mg/g) | $b$ | $R^2$ (L/mg) | $K_f$ (mg/g) | $n$ | $R^2$ (L/mg) | $K_t$ | $B$ | $R^2$ |
| Cu(II) | 181.81 | 18.33 | 0.99 | 194.02 | 38.31 | 0.87 | $9.39 \times 10^{16}$ | −4.97 | 0.99 |
| Pb(II) | 88.49 | 0.23 | 0.95 | 229.72 | 5.66 | 0.71 | 5309.749 | −25.332 | 0.79 |

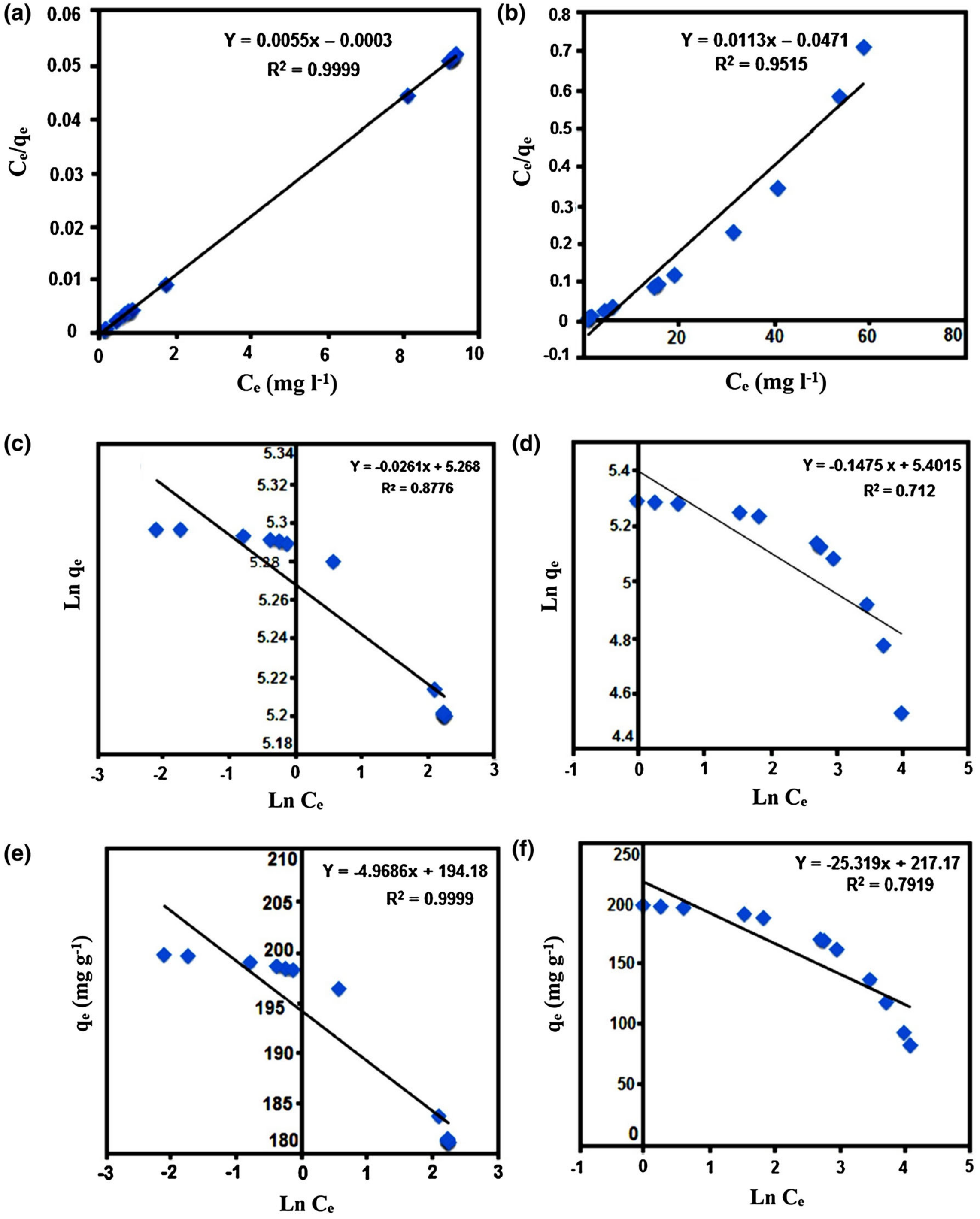

**Fig. 8** Langmuir [**a** Cu(II) and **b** Pb(II)], Freundlich [**c** Cu(II) and **d** Pb(II)] and Temkin [**e** Cu(II) and **f** Pb(II)] isotherms for heavy metals adsorption onto MDA-MCN-1

**Table 4** Comparison of the heavy metals adsorption by functionalized mesoporous carbon nitride in this study with various related substances from the literature

| Adsorbent | | Adsorbent dose (mg/L) | Metal conc. (mg/L) | Type | pH | Adsorption capacity (mg/g) | | References |
|---|---|---|---|---|---|---|---|---|
| Mesopore | Ligand | | | | | Pb(II) | Cu(II) | |
| SBA-15 | *N*-3-(trimethoxysilyl)-propyldiethylenetriamine | 1.1 | 113 | Single | – | – | 9.4 | Aguado et al. (2009) |
| SBA-15 | Trimethoxysilylpropyldiethylenetriamine | 10 | 11 | Single | – | 1.1 | 1.0 | Zhang et al. (2007) |
| SBA-15 | *N*-propylsalicylaldimine | 1 | 318 | Mixed | 4.8 | – | 57.2 | Mureseanu et al. (2008) |
| SBA-16 | 3-Mercaptopropyltriethoxysilane | 5 | 127 | Single | 5 | – | 36.4 | Xue and Li (2008) |
| MCM-41 | 3-Aminopropytriethoxysilane | 5 | 50 | Mixed | 5 | 57.7 | – | Heidari et al. (2009) |
| SBA-15 | 3-Aminopropytriethoxysilane | 2 | 100 | Single | 4 | 23.7 | 19.4 | Shahbazi et al. (2011) |
| SBA-15 | Melamine-based $NH_2$ dendrimer | 1 | 100 | Single | 4 | 94.8 | 90.3 | Shahbazi et al. (2011) |
| MCN-1 | Melamine-based dendrimer amine | 0.5 | 100 | Single | 8 | 196.34 | 199.75 | This study |

affinity to the metal governs the adsorption process, but when presumably the metal cation concentration increased, this site becomes saturated, and then, the amine groups in MCN-1 surface govern the adsorption. The values of $n$ are $>1$ (5.66–38.31), it is indicative of high adsorption intensity (Benhamou et al. 2009). On the other hand, the adsorption affinity and adsorption energy increased as follows, Cu(II) > Pb(II), with similar increase in the $n$ and $b$ values in the Freundlich and Langmuir isotherm models. The adsorption results were compared with those of mesoporous based adsorbents, reported by other authors (Table 4), and this reveals that the adsorption efficiency of the dendrimer amine functionalized MCN-1 prepared in this work is generally higher than the previously reported values.

### *Adsorption kinetics*

The study of adsorption kinetics is significant as it provides valuable insights into the reaction pathways and the mechanism of the reactions. Any adsorption process is normally controlled by the three diffusion steps: transport of the solute (1) from bulk solution to the film surrounding the adsorbent, (2) from the film to the adsorbent surface, and (3) from the surface to the internal sites followed by binding of the metal ions to the active sites. The slowest steps determine the overall rate of the adsorption process, and usually, it is thought that step (2) shows the surface adsorption step of Pb(II) and Cu(II) ions and step (3) shows the intra-particle adsorption of Pb(II) and Cu(II) ions (Sharma and Bhattacharyya 2004). Several kinetic models are used to explain the mechanism of the adsorption processes. A simple pseudo-first-order equation is given by Lagrange equation (Ho et al. 2000):

$$\ln(q_e - q_t) = \ln q_e - K_1 t \tag{10}$$

where $q_e$ and $q_t$ are the amounts of Cu(II) and Pb(II) adsorbed (mmol/g) at equilibrium time and any time t, respectively, and $K_1$ is the rate constant of adsorption ($\mathrm{min}^{-1}$). Plot of $\log(q_e - q_t)$ versus $t$ gives a straight line for first-order adsorption kinetics, which allows computation of the rate constant $K_1$. The calculated $q_e$, $K_1$ and the corresponding linear regression correlation coefficient values are summarized in Table 5. It is clear from Table 4 that the calculated linear regression correlation coefficient ($R^2$) is relatively small (0.3 and 0.94, respectively), and the experimental $q_e$ values do not agree with the calculated values obtained from the linear plots. The pseudo-second-order equation based on equilibrium adsorption is expressed as (Sharma and Bhattacharyya 2004):

$$\frac{t}{q_t} = \frac{1}{K_2 q_e^2} + \frac{t}{q_e} \tag{11}$$

where $K_2$ is the pseudo-second-order rate constant (g/mmol min), and $q_e$ and $q_t$ represent the amount of Cu(II) and Pb(II) adsorbed (mmol/g) at equilibrium and at any time. The equilibrium adsorption capacity ($q_e$) and the second-order constants ($K_2$) can be determined experimentally from the slope and intercept of plot $\frac{t}{q_t}$ versus $t$ (Fig. 9). The calculated $q_e$, $K_2$ and the corresponding linear regression correlation coefficient values are summarized in Table 4.

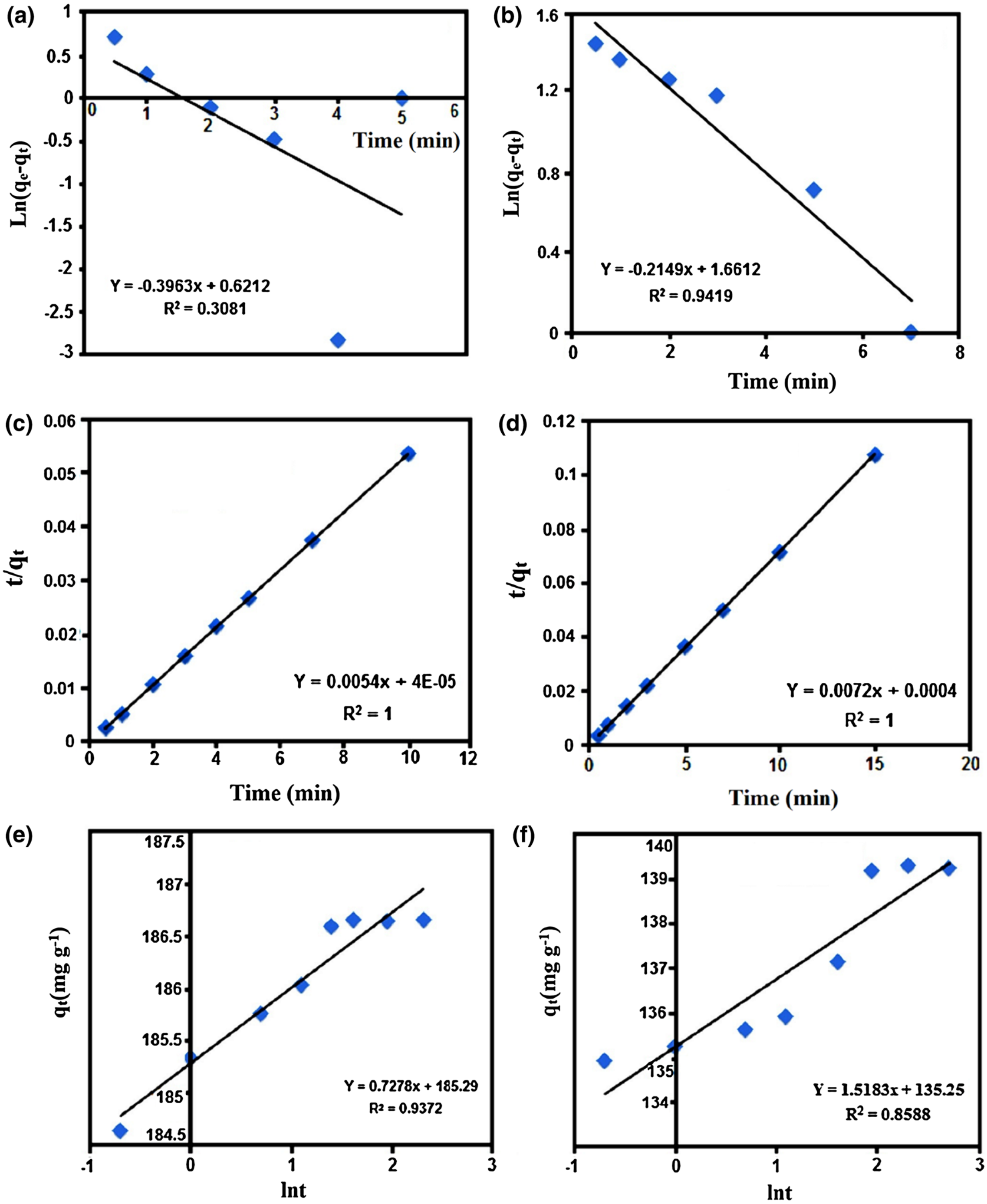

**Fig. 9** Pseudo-first-order [**a** Cu(II) and **b** Pb(II)], pseudo-second-order [**c** Cu(II) and **d** Pb(II)] and Elovich [**e** Cu(II) and **f** Pb(II)] kinetics models of heavy metals adsorption onto MDA-MCN-1

The adsorption rate is related to the content of the active adsorption sites on the matrix of the adsorbent and also on the metal ionic radius (Jing et al. 2009). According to Table 4, Cu(II) ions with a lower ionic radius show higher adsorption rate. The reason for this may be due to the fact that the Cu(II) ions win over in the competition for occupying the active sites on the adsorbent surface.

A simplified linearized form of Elovich kinetic equation is presented as follows:

$$q_t = \frac{1}{\beta}\ln(\alpha\beta) + \frac{1}{\beta}\mathrm{lnt} \tag{12}$$

where a (mg/g min) is the initial adsorption rate and b is related to the extent of surface coverage and the activation

**Table 5** Pseudo-first-order, pseudo-second-order and Elovich constants for the removal of Pb(II) and Cu(II) metal ions by MDA-MCN-1

| Metals | Pseudo-first-order constants | | | Pseudo-second-order constants | | | Elovich | | |
|---|---|---|---|---|---|---|---|---|---|
| | $q_e$ (mg/g) | $K_1$ | $R^2$ (L/mg) | $q_e$ (mg/g) | $K_2$ | $R^2$ (L/mg) | α mg ($g^{-1}$/min) | β (g/mg) | $R^2$ |
| Cu(II) | 1.86 | 0.39 | 0.30 | 185.18 | 0.72 | 0.997 | $2.68 \times 10^{110}$ | 1.37 | 0.94 |
| Pb(II) | 5.26 | 0.21 | 0.94 | 138.88 | 0.12 | 0.981 | $7.38 \times 00^{38}$ | 0.66 | 0.86 |

**Table 6** Adsorption–desorption data in consecutive cycles

| Cycle | Pb(II) adsorption capacity | | Pb(II) desorption | | Cu(II) adsorption capacity | | Cu(II) desorption | |
|---|---|---|---|---|---|---|---|---|
| | $C_0$ (mg/L) | $q_e$ (mg/g) | $C_0$ (mg/L) | % desorption | $C_0$ (mg/L) | $q_e$ (mg/g) | $C_0$ (mg/L) | % desorption |
| 1 | 100 | 196.34 | 97.42 | 97.42 | 100 | 199.75 | 98.26 | 98.26 |
| 2 | 97.42 | 190.44 | 95.64 | 98.17 | 98.26 | 194.82 | 96.78 | 98.49 |
| 3 | 95.64 | 188.27 | 94.13 | 98.42 | 96.78 | 191.36 | 95.25 | 98.41 |
| 4 | 94.13 | 185.12 | 92.36 | 98.11 | 95.25 | 189.12 | 93.82 | 98.49 |

energy involved in chemisorption (g/mg) (Zhang et al. (2010).

As recorded in Table 5, the values of $q_e$ calculated from pseudo-second-order kinetics almost agreed well with the experimental values of $q_e$. The results presented in Fig. 9 shows that the pseudo-second-order was able to provide better fit ($R^2 = 1$ compared with $R^2 = 0.3081$–$0.9419$ for pseudo-first-order kinetics and $R^2 = 0.9372$–$0.8588$ for the Elovich). These results and the values of $R^2$ indicate that the adsorption of Cu(II) and Pb(II) ions on the prepared mesoporous carbon follow pseudo-second-order kinetics. A small pore diameter and a small pore volume are favorable to a higher adsorption capacity, and a better pore connectivity provides a higher adsorption rate.

### *Desorption and reusability studies*

The important factor in the adsorption process is regeneration of the adsorbent for repeated use. The desorption of adsorbed Pb(II) and Cu(II) was studied using 0.1 MHNO$_3$. The results of adsorption of MDA-MCN-1 for four consecutive adsorption–desorption cycles are presented in Table 6. These results indicated that, after four consecutive cycles of adsorption–desorption, the adsorption capacity of Pb(II) and Cu(II) decreased slightly. The main reason for this result is attributed to the ordered structure of the porous adsorbents.

## Conclusion

The mesoporous carbon nitride (MCN-1) with high thermal stability, high surface area and large pore volumes has been synthesized. Then, dendrimer amine-grafted mesoporous carbon nitride (MDA-MCN-1) is prepared by a post-grafting process. Their structures have been characterized by means of FTIR spectroscopy, thermogravimetric analysis, nitrogen adsorption–desorption and small-angel X-ray scattering. MDA-MCN-1 has been employed to study the removal of Pb(II) and Cu(II) ions from aqueous solution by using batch system, and has been found to be effective adsorbent than others. This melamine-based dendrimer exhibits high efficiency for heavy metals removal in aqueous media in the order of Cu(II) > Pb(II). On the other hand, the binding preference of the heavy metals is attributed to their atomic properties and also to the chemistry of the solution such as the pH. The optimum pH value for the removal of the studied ions by MDA-MCN-1 from aqueous solution was pH 8. Higher adsorption capacity is obtained at 20 °C and decreases with increase in temperature. The Langmuir isotherm fitted the equilibrium data better than the Freundlich isotherm, with a higher correlation coefficient. The pseudo-first-order and pseudo-second-order kinetic models have been used to analyze the data obtained for Pb(II) and Cu(II) adsorption on the MDA-MCN-1. The results exhibit that the pseudo-second-order equation provides the better correlation for the adsorption data.

**Acknowledgments** The authors are thankful to Research Council of Iran University of Science and Technology (Tehran) for financial support to this study.

## References

Abdel-Ghani NT, Elchaghaby GA (2007) Influence of operating conditions on the removal of Cu, Zn, Cd and Pb ions from wastewater by adsorption. Int J Environ Sci Technol 4:451–456

Acosta EJ, Carr CS, Simanek EE, Shantz DF (2004) Engineering nanospaces: iterative Synthesis of melamine-based dendrimers on amine-functionalized sba-15 leading to complex hybrids with controllable chemistry and porosity. Adv Mater 16:985–989

Acosta EJ, Gonzalez SO, Simanek EE (2005) Synthesis, characterization, and application of melamine-based dendrimers supported on silica gel. Part A Polym Chem 43:168–177

Aguado J, Arsuaga JM, Arencibia A, Lindo M, Gascón V (2009) Aqueous heavy metals removal by adsorption on amine-functionalized mesoporous silica. J Hazard Mater 163:213–221

Amini M, Younesi H, Bahramifar N (2009) Statistical modeling and optimization of the cadmium biosorption process in an aqueous solution using *Aspergillus niger*. Colloids Surf Physicochem Eng Aspects 337:67–73

Anbia M, Ghaffari A (2009) Adsorption of phenolic compounds from aqueous solutions using carbon nanoporous adsorbent coated with polymer. Appl Surf Sci 255:9487–9492

Anbia M, Ghassemian Z (2011) Removal of Cd(II) and Cu(II) from aqueous solutions using mesoporous silicate containing zirconium and iron. Chem Eng Res Des 89:2770–2775

Anbia M, Habibi Davijani A (2013) Synthesis of L-cysteine grafted nanoporous carbon (CMK-3) and its use as a new cadmium sorbent. Chem Eng J 223:899–907

Anbia M, Hoseini V (2012) Enhancement of $CO_2$ adsorption on nanoporous chromium terephthalate (MIL-101) by amine modification. J Nat Gas Chem 21:339–343

Anbia M, Moradi SE (2009) Removal of naphthalene from petrochemical wastewater streams using carbon nanoporous adsorbent. Appl Surf Sci 255:5041–5047

Anbia M, Parvin Z (2011) Desulfurization of fuels by means of a nanoporous carbon adsorbent. Chem Eng Res Des 89:641–647

Anbia M, Mohammadi N, Mohammadi K (2010) Fast and efficient mesoporous adsorbents for the separation of toxic compounds from aqueous media. J Hazard Mater 176:965–972

Ansari MB, Jin H, Parvin MN, Park SE (2012) Mesoporous carbon nitride as a metal-free base catalyst in the microwave assisted Knoevenagel condensation of ethylcyanoacetate with aromatic aldehydes. Catal Today 185:211–216

Antochshuk V, Jaroniec M (2002) 1-Allyl-3-propylthiourea modified mesoporous silica for mercury removal. Chem Commun 3:258–259

Benhamou A, Baudu M, Derriche Z, Basly JP (2009) Aqueous heavy metals removal on amine-functionalized Si-MCM-41 and Si-MCM-48. J Hazard Mater 171:1001–1008

Bodek I, Lyman WJ, Reehl WF, Rosenblatt DH (1998) Environmental inorganic chemistry: properties, processes and estimation methods. Pergamon Press, New York

Chew TL, Ahmad AL, Bhatia S (2010) Ordered mesoporous silica (OMS) as an adsorbent and membrane for separation of carbon dioxide ($CO_2$). Adv Colloid Interface Sci 153:43–57

Colilla M, Balas F, Manzano M, Vallet-Regı M (2008) Novel method to synthesize ordered mesoporous silica with high surface areas. Solid State Sci 10:408–415

Datta KKR, Balasubramanian VV, Ariga K, Mori T, Vinu A (2011) Highly crystalline and conductive nitrogen-doped mesoporous carbon with graphitic walls and its electrochemical performance. Chem Eur J 17:3390–3397

Gavrilescu M (2004) Removal of heavy metals from the environment by biosorption. Eng Life Sci 4:219–232

Gercel Ö, Gerc HF (2007) Adsorption of lead (II) ions from aqueous solutions by activated carbon prepared from biomass plant material of Euphorbia rigida. Chem Eng J 132:289–297

Gillan EG (2000) Synthesis of nitrogen-rich carbon nitride networks from an energetic molecular azide precursor. Chem Mater 12:3906–3912

Groenewolt M, Antonetti M (2005) Synthesis of g-C3N4 nanoparticles in mesoporous silica host matrices. Adv Mater 17:1789–1792

Heidari A, Younesi H, Mehraban Z (2009) Removal of Ni(II), Cd(II), and Pb(II) from a ternary aqueous solution by amino functionalized mesoporous and nano mesoporous silica. Chem Eng J 153:70–79

Ho YS, Ng JCY, McKay G (2000) Kinetics of pollutant sorption by biosorbents: review. Sep Purif Methods 29:189–232

Iijima S (1991) Helical microtubules of graphitic carbon. Nature 354:56–58

Jiang Y, Gao Q, Yu H, Chen Y, Deng F (2007) Intensively competitive adsorption for heavy metal ions by PAMAM–SBA-15 and EDTA–PAMAM–SBA-15 inorganic-organic hybrid materials. Microporous Mesoporous Mater 103:316–324

Jin X, Balasubramanian VV, Selvan ST, Sawant DP, Gari MA, Lu GQ, Vinue A (2009) Highly ordered mesoporous carbon nitride nanoparticles with a high nitrogen content: a novel metal-free basic catalyst. Angew Chem Int Ed 48:7884–7887

Jing X, Liu F, Yang X, Ling P, Li L, Long C, Li A (2009) Adsorption performances and mechanisms of the newly synthesized N, *N*-di (carboxymethyl) dithiocarbamate chelating resin toward divalent heavy metal ions from aqueous media. J Hazard Mater 167:589–596

Júnior OK, Gurgel LVA, de Freitas RP, Gil LF (2009) Adsorption of Cu(II), Cd(II), and Pb(II) from aqueous single metal solutions by mercerized cellulose and mercerized sugarcane bagasse chemically modified with EDTA dianhydride (EDTAD). Carbohydr Polym 77:643–650

Kawaguchi M, Yagi S, Enomoto H (2004) Chemical preparation and characterization of nitrogen-rich carbon nitride powders. Carbon 42:345–350

Khabashesku VN, Zimmerman JL, Margrave JL (2000) Powder synthesis and characterization of amorphous carbon nitride. Chem Mater 12:3264–3270

Kouvetakis J, Bandari A, Todd M, Wilkens B, Cave N (1994) Novel synthetic routes to carbon-nitrogen thin films. Chem Mater 6:811–814

Kroke E, Schwarz M (2004) Novel group 14 nitrides. Coord Chem Rev 248:493–532

Liang Z, Fadhel B, Schneider CJ, Chaffee AL (2008) Stepwise growth of melamine-based dendrimers into mesopores and their $CO_2$ adsorption properties. Microporous Mesoporous Mater 111:536–543

Lu AH, Schuth F (2005) Nanocasting pathways to create ordered mesoporous solids. C R Chim 8:609–620

Mureseanu M, Reiss A, Stefanescu I, David E, Parvulescu V, Renard G, Hulea V (2008) Modified SBA-15 mesoporous silica for heavy metal ions remediation. Chemosphere 73:1499–1504

Olkhovyk O, Jaroniec M (2005) Adsorption characterization of ordered mesoporous silicas with mercury-specific immobilized ligands. Adsorption 11:685–690

Qiu Y, Gao L (2003) Chemical synthesis of turbostratic carbon nitride, containing C-N crystallites, at atmospheric pressure. Chem Commun 18:2378–2379

Rangel-Mendez JR, Streat M (2002) Adsorption of cadmium by activated carbon cloth: influence of surface oxidation and solution pH. Water Res 36:1244–1252

Reddad Z, Gerente C, Andres Y (2002) Adsorption of several metal ions onto a low-cost biosorbent: kinetic and equilibrium studies. Environ Sci Technol 36:2067–2073

Selvam P, Bhatia SK, Sonwane CG (2011) Recent advances in processing and characterization of periodic mesoporous MCM-41 silicate molecular sieves. Ind Eng Chem Res 40:3237–3261

Shahbazi A, Younesi H, Badiei A (2011) Functionalized SBA-15 mesoporous silica by melamine-based dendrimer amines for adsorptive characteristics of Pb(II), Cu(II) and Cd(II) heavy metal ions in batch and fixed bed column. Chem Eng J 168:505–518

Sharma A, Bhattacharyya KG (2004) Adsorption of chromium (VI) on Azadirachta Indica (Neem) leaf powder. Adsorption 10:327–338

Song L, Zhang S, Wu X, Wei Q (2012) A metal-free and graphitic carbon nitride sonocatalyst with high sonocatalytic activity for degradation methylene blue. Chem Eng J 184:256–260

Thomas A, Fischer A, Goettmann F, Antonietti M, Müller JO, Schlogl R, Carlsoon JM (2008) Graphitic carbon nitride materials: variation of structure and morphology and their use as metal-free catalysts. J Mater Chem 18:4893–4908

Tomalia DA, Naylor AM, Goddard WA (1990) Starburst dendrimers: molecular-level control of size, shape, surface chemistry, topology, and flexibility from atoms to macroscopic matter. Angew Chem Int Ed 29:138–175

Vinu A, Ariga K, Mori T, Nakanishi T, Hishita S, Golberg D, Bando Y (2005) Preparation and characterization of well-ordered hexagonal mesoporous carbon nitride. Adv Mater 17:1648–1652

Vinu A, Srinivasu P, Sawant DP, Mori T, Ariga K, Chang J, Jhung S, Vaithilingam Balasubramanian V, Hwang YK (2007a) Three-dimensional cage type mesoporous cn-based hybrid material with very high surface area and pore volume. Chem Mater 19:4367–4372

Vinu A, Mori T, Hishita S, Anandan S, Balasubramanian VV, Ariga K (2007b) One and three dimensional mesoporous carbon nitride molecular sieves with tunable pore diameters. Stud Surf Sci Catal 165:905–908

Wang SY, Tsai MH, Lo SF, Tsai MJ (2008) Effects of manufacturing conditions on the adsorption capacity of heavy metal ions by Makino bamboo charcoal. Bioresour Technol 99:7027–7033

Xue X, Li F (2008) Removal of Cu(II) from aqueous solution by adsorption onto functionalized SBA-16 mesoporous silica. Microporous Mesoporous Mater 116:116–122

Yang Z, Xia Y, Mokaya R (2005) Hollow shells of high surface area graphitic N-doped carbon composites nanocast using zeolite templates. Microporous Mesoporous Mater 86:69–80

Yazdankhah A, Moradi SE, Amirmahmoodi S, Abbasian M, Esmaeily Shoja S (2010) Enhanced sorption of cadmium ion on highly ordered nanoporous carbon by using different surfactant modification. Microporous Mesoporous Mater 133:45–53

Yuan X, Zhuo SP, Xing W, Cui HY, Dai XD, Liu XM, Yan ZF (2007) Aqueous dye adsorption on ordered mesoporous carbons. J Colloid Interface Sci 310:83–89

Zhang W, Simanek EE (2000) Dendrimers based on melamine. Divergent and orthogonal, convergent syntheses of a G3 dendrimer. Org Lett 2:843–845

Zhang W, Simanek EE (2001) Synthesis and characterization of higher generation dendrons based on melamine using *p*-aminobenzylamine. Evidence for molecular recognition of Cu(II). Tetrahedron Lett 42:5355–5357

Zhang L, Yu C, Zhao W, Hua Z, Chen H, Li L, Shi J (2007) Preparation of multiamine-grafted mesoporous silicas and their application to heavy metal ions adsorption. J Non Cryst Solids 353:4055–4061

Zhang Y, Li Y, Yang LQ, Ma XJ, Wang LY, Ye ZF (2010) Characterization and adsorption mechanism of $Zn^{2+}$ removal by PVA/EDTA resin in polluted water. J Hazard Mater 178:1046–1054

Zheng Z, Gao Q, Jiang J (2010) High hydrogen uptake capacity of mesoporous nitrogen-doped carbons activated using potassium hydroxide. Carbon 48:2968–2973

Zimmerman JL, Williams R, Khabashesku VN, Margrave JL (2001) Synthesis of spherical carbon nitride nanostructures. Nano Lett 12:731–734

Zolfaghari G, Esmaili-Sari A, Anbia M, Younesi H, Amirmahmoodi S, Ghafari-Nazari A (2011) Taguchi optimization approach for Pb(II) and Hg(II) removal from aqueous solutions using modified mesoporous carbon. J Hazard Mater 192:1046–1055

Zvinowanda CM, Okonkwo JO, Shabalala PN, Agyei NM (2009) A novel adsorbent for heavy metal remediation in aqueous environments. Int J Environ Sci 6:425–434